Czesław GARBALEWSKI
Polish Academy od Sciences
Institute of Oceanology — Sopot

MEAN SPATIAL DISTRIBUTION OF BASIC PHYSICAL CHARACTERISTICS AND SOURCE REGIONS OF PARTICLE EMISSION FROM THE OCEAN SURFACE*

1. INTRODUCTION

1.1. Source and sink regions

In the general macroscale water circulation mechanism attention should be paid to the exchange of the dispersed mass systems between the sea and the atmosphere. This exchange, occurring simultaneously in the two opposite vertical directions, is characterized by the occurrence of relative source and sink regions of particle transfer. These areas were described by Eriksson [10] when considering the influence of circulation upon the residence time of the substance components in the atmosphere. One may assume that relative to the globe, the land and the sea are first-grade sink regions for the seaborne suspensions and aerosols originating from the land, respectively. The aim of the present study is to obtain the space-time distribution of the regions of aerosol exchange occurring within the boundaries of the World Ocean surface. These are the second-grade source and sink areas, i.e., relative regions of the vertical particulate exchange above the ocean.

The investigation of the macroscale distribution of relative source and sink areas in respect of marine particle transfer is essential for the explanation and assessment of the share of particular components of the

* Carried out under Inter-ministerial programme I/15 coordinated by the Polish Academy of Sciences.

water budget and the circulation of pollution in geochemical cycles. It is also possible to determine the share of individual seas in the total transfer. Among other things, this also concerns the Baltic Sea, the place and share of which in the general spatial distribution of emission and transfer is one of the most important problems discussed in this paper.

The present investigations did not cover the influence of the surf-effect on the emission fields. The participation of this effect should necessitate the introduction of the correction coefficient when calculating the emission fields in coastal zones, as well as in the regions of the marked occurrence of icebergs. However, the determination of the magnitudes of this coefficients, depending, among other things, on the geommetry of the shores and the surf regions, is a problem that has not been explained so far. One may also expect some deviations from the mean sea-drop emission field along the path of tropical cyclones. These deviations may be due to the increased share of additional emission mechanisms during hurricanes. Tropical cyclones are relatively rare however, and travel along narrow paths only, while the participation of large and rapid fall-out of seaborne drops in long-term exchange, i.e. in particle circulation during synoptic and macroscale cycles, is too small to consider. These problems require more detailed investigations, but a general view is also valuable.

1.2. Investigations of the emission mechanism

Transfer of suspended systems over the sea surface is worth consideration, being one of the forms of the exchange of energy and mass between the sea and the atmosphere. Interest in the problem increased with the development of investigations in the field of the physics of the interaction between the sea and atmosphere. For the first time, Woodcock [32] investigated the dependence of emission and transfer of sea-salt particles, being marine condensation nuclei, on wind velocity over the ocean surface. The essential role of air bubbles and sea foam in the mechanism of the emission of water drops from the sea was explained by Blanchard, Kientzler, Woodcock and others [1, 3, 14, 21, 26, 31]. Blanchard [2] compared the efficiency of the emission of drops from the open sea with that in the coastal zone, characteristic of stormy mutual interaction of waves and steep shores. The related differences in the chemical composition of the particles emitted were studied by Duce and Woodcock [9]. Blinov [5] pointed to the significant share in suspension due to splashes which were directly blown off the wave crests by strong gusts of wind in the open sea. Simultaneously, Woodcock [32]

investigated the distribution of the size of sea-salt particles while Junge [15, 16] explained the law of the distribution of aerosol particles and compared the dispersive characteristics of aerosols of sea- and land--origin. Moore and Mason [23] investigated the size distribution of marine particles as related to the source efficiency.

The results mentioned, as well as papers [4, 12, 18, 22, 27, 32] concerning the distribution and dynamics of sea-salt particles concentration in the air, supplemented by model investigations of the emission and transfer processes [27, 29, 30, 34], helped to verify the opinion as to the factors forming the emission of drops from the sea. In general, this opinion is consistent with the concept [12] of the predominating influence of the basic characteristics of mechanical interaction between the atmosphere and the sea, i.e. roughness length and the Reynolds stresses, on the energy dissipation and aerosol mass exchange. As a result, a model was obtained, which gave an approximate description of particle emission rate from the sea. In the present paper, this concept was assumed to be fundamental in order to solve the problem of the spatial distribution of the basic characteristics of the emission of drops from the sea surface.

2. THEORY

The air-sea system in which the processes of the transformation of gas bubbles into water drops above the sea surface occur will be termed the marine aerosol production layer. The production layer that is statistically homogeneous in the horizontal plane, is characterized by anisotropy due to several sublayers occurring in its microstructure. Together they form two essentially different sublayers — the emission and the transport sublayers (Fig. 1).

The evolution of gas bubbles and the emission of drops accompanying the bursting of bubbles at the sea surface, take place in the emission sublayer. The emission of bubbles occurs in the near-surface sea layer where the forming of bubbles is affected by the process of the wind-waves breaking. This influence reaches a depth $-h_1$ corresponding to the thickness of the near-surface sublayer. Simultaneously, the efficiency of the emission of drops and bursting of bubbles is influenced by the laminar sublayer thickness ($-\delta_v$) restraining the motion of particles in the sea, and by the monomolecular surface film [13] with a thickness of $-\delta_o$, the surface tension being σ_m. An important role in the mechanism of the evolution of bubbles and the emission of drops, is played by the intensity of air exchange with the water body. This

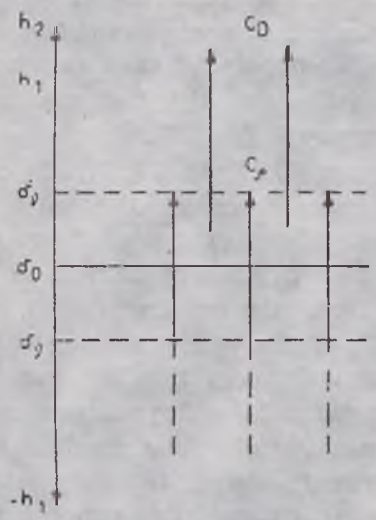

Fig. 1. Vertical profile of the marigenic aerosol production layer at the air-sea interface
$-h_1$, $-\delta_o$, $-\delta_v$ are: the depth of the near-surface layer, the thicknesses of laminar sublayer, and surface film, respectively,
δ_v, h_1 are: thicknesses of the molecular viscous and dynamic sublayers forming the near-water atmospheric layer with the thickness of h_2.
Rys. 1. Schemat pionowego przekroju warstwy produkcji aerozolu marygenicznego
$-h_1$, $-\delta_v$, $-\delta_o$ — odpowiednio: głębokość przypowierzchniowej podwarstwy morza, grubości warstwy laminarnej i monomolekularnej warstwy powierzchniowej,
δ_v, h_1 — odpowiednio: grubości podwarstw lepkości molekularnej i dynamicznej w składzie przywodnej warstwy atmosfery o grubości h_2.

exchange depends upon the thickness of the viscous sublayer of air, (δ_v), in the near-water atmospheric layer (stretching up to a height of h_2), as well as on the ratio of this thickness to the variable value of roughness length (z_o) for the sea surface.

The thickness of the molecular viscosity sublayer, δ_v is also a component of the transfer sublayer characteristics, as fluctuations in the concentration of seaborne particles in the near-water atmospheric layer are connected with the transport of drops at its lowest levels. These fluctuations depend on the variable conditions of emission, as well as on the microstructure of the turbulent dynamic sublayer reaching a height of h_1. On the one hand, it is connected with the dynamics of the interaction between the sea surface and the near-water air layer, and on the other hand — with turbulent mixing in near-water air.

Taking into account the influence of the wind velocity (u), and the Reynolds number (Re_s) in the near-wall layer, Garbalewski [12] proposed the following relation for the flux of dust emission from the sea surface:

$$Q_0 = k\, u\, Re_s\, S_m \qquad (1)$$

After some modifications, when taking into account the logarithmic law of the wind velocity distribution related to height, equation (1) becomes:

$$Q_0 = c_\varrho S_m \frac{u_*^2 z_0}{\nu} + \delta \quad , \quad z = \text{const} \qquad (2)$$

where $Re_s = \frac{u_* z_o}{\nu}$, u_* — the friction velocity, z_o — the roughness length, ν — the kinematic molecular viscosity, $S_m = \varrho_w q_n$, ϱ_w — density of water in the surface sea layer, q_n — share of the mass of the n-th sea water component, c_ρ — the drag coefficient for the particle emission, δ — a small part of the particle mass q_n — escaping from the sea with the evaporation of water. Equation (2) describes the emission conditions at height z_o.

Proposed relation (1) may be justified theoretically. Accordingly, the c_ρ coefficient, analogical to the Dalton number for humidity, may be written as:

$$c_\rho = \frac{Q_0}{\varrho\, q_n\, u_0} \qquad (3)$$

Integrating the Boussinesq equation

$$u_*^2 = \nu \frac{\partial u}{\partial z} \qquad (4)$$

for $z = z_o$ we obtain

$$u_0 = \frac{u_*^2 z_0}{\nu} \qquad (5)$$

where u_o is the modulus of the wind velocity measured at a height z_o with respect to the water surface. It should be emphasized that in the wind profile at the viscous sublayer level, $\delta\nu$, where direct interaction between the wind and the rough sea surface occurs, one usually assumes that for the sea $u_o > 0$. Substitution of the u_o value from relation (5) to (3) yields equation (2), i.e. the transformation of the proposed relation (1).

The concept of the two-stage structure of the production layer implies that in general approximation, the particle emission flux at level z can be described by the equation:

$$Q_z = k S_m \frac{u_*^2 z_0}{\nu} + \delta \quad , \quad z = \text{const} \qquad (6)$$

where $k = c_\rho c_D$

i.e. a product of the drag coefficients, both for the emission at the z_o level and the particle separative transfer at level z, respectively. The flux of particles carried to level z is influenced by Q_o and may be expressed as:

$$Q_z = c_D Q_0$$

Analytical determination of the complex drag parameter, k, is difficult, mainly due to the c_ϱ parameter being one of the k components. The c_ϱ parameter characterizes the complex transformation sublayer of the dispersed systems. The characteristics of this sublayer determine the amount of work needed to overcome the resistance when drops permeate through both laminar sublayers, $-\delta_v$ and δ_v and the surface film $-\delta_o$. An important role is also played by the film thickness and the surface tension. Variable conditions of gas bubble formation in the water body are of additional importance. The theory of the near-wall biphase layer and the analogy between the emission process and the hydrodynamics of bubbling and barbotage [19] give:

$$c_\varrho = \frac{v_{kr}\sqrt{\varrho_p}}{\sqrt[4]{g\,\sigma_m(\varrho_w - \varrho_p)}} \qquad (7)$$

where v_{kr} — the critical velocity of the gas bubble ascent in the water body, measured with respect to the water, and determination of the condition of the surface film bursting, ϱ_p and ϱ_w — the air and water densities, respectively, g — gravity, σ_m — sea surface tension. Unstabilized gas pressure on the surface film is the factor which disturbes the equilibrium between the two phases, the pressure related to the surface tension σ_m being the stabilizing factor.

The c_D value should vary depending on the size distribution of the emitted particles, as well as on the velocity of their separative fall out. For small particles characterized by low Re_s values, the acceleration due to inertial forces can be omitted. The fall out of such particles is determined by the displacement and viscosity forces. According to the theory of similarity, the resultant velocity of their fall out corresponds to the velocity scale:

$$v_d \sim \frac{g' d^2}{\nu} \qquad (8)$$

where $g' = g\,\frac{\varrho'}{\varrho_o}$ is the balanced gravity, ϱ' and ϱ_o — the densities in the isothermally stratified and in average atmosphere, respectively. The finite particle residence time in the air can be determined where there is a lack of equilibrium between v_d and the diffusion rate vertical component w, i.e. where the following relation is fulfilled:

$$\frac{\partial n(d)}{\partial t} = \frac{\partial}{\partial z}\left[D \frac{\partial n(d)}{\partial z} - v_d n(d) \right] \qquad (9)$$

where $n(d)$ — the number of particles with a diameter d, D — the diffusion coefficient. In the viscous sublayer this time amounts to

$$\tau_0 = \frac{z_0}{v_{d_0}}$$

with $\delta v \sim z_0$, and in the dynamic sublayer

$$\tau_1 = \frac{z_1}{v_{d_1}}$$

Due to the different dispersion composition of the suspensions at heights z_0 and z_1 the mean spectral value of the diameter $\bar{d}_0 > \bar{d}$ and $v_{d0} > v_d$, hence $\tau_0 \ll \tau_1$.

An equation describing the volume concentration of the mass of emitted suspension in the air can be obtained from relation (2) for the emission conditions at level $z = z_0$:

$$q_z = k \xi_z \varrho_w q_n \quad , \quad z = \text{const} \qquad (10)$$

where $\xi_z = \frac{u_*^2 z_0}{u_z \nu}$ denotes a dimensionless dynamic factor which is the ratio of Re_s and M, where $M = \frac{u_z}{u_*}$. Hence, the drag coefficient is expressed by

$$c_D = \frac{\xi_z}{\xi_0} = \frac{u_0}{u_z} \qquad (11)$$

where ξ_0, ξ_z, and u_0, u_z are the values of the dimensionless dynamic factor and the wind velocity modulus for level z_0 and height z above the sea surface, respectively.

As the flux $Q = qw$, where $w = \frac{z}{\tau}$ is the vertical component of the diffusion rate and τ is the time for which particles remain in the air on reaching height z, the ratio may be written as

$$\frac{Q_z}{Q_0} = c_D^2 \frac{\tau_0 z}{\tau_z z_0} \qquad (12)$$

Hence, the formula for the drag coefficient related to the separative transport of marine particle suspension can be expressed as a ratio of the vertical diffusion rates at level z_o and height z:

$$c_D = \frac{w_0}{w_z} \quad (13)$$

In principle, expression (10) takes into account the deviation of true wind velocities ($\frac{u}{u_*}$) from those obtained from the law of logarithmic distribution depending on height ($\frac{u_* z_o}{\nu}$). The dimensionless dynamic factor ξ'_z is a measure of the deviation of true conditions from the logarithmic distribution, as well as that of the deviation from the smooth surface conditions, being a complex value which at level z=const is, in principle, a function of the Reynolds and Richardson numbers:

$$\xi'_{z=\text{const}}(Re_s, Ri) = k\,\xi_z \quad (14)$$

Thus, indirectly, the expression also takes into account the influence of atmospheric equilibrium on the changes in the concentration of particles carried away from the sea. For the particle emission at level $z = z_o$, this influence in equation (2) leads mainly to the influence of the friction velocity and the Reynolds number.

3. METHODS

For the computations of the anemoaerosol emission fields, mean data obtained over a period of many years for a standard height of 10 m above the sea level contained in climatological summaries and marine atlases [20, 24], were used. On such bases, tables were prepared: for the wind velocities (u_i) and the frequencies of their occurrence for the i-th direction, for the air and sea temperatures near their interface, and for the water density and salinity — for a network of points with given geographical coordinates. Mean ϱ_p values were taken from tables [17] for the level $z = 0$ km according to the zones of geographical latitudes for quarterly periods. The ν values were calculated corresponding to the air temperature at 5°C intervals. The wind velocity was computed from the Beaufort wind force scale, the computations being carried out on the bases of established equivalent velocity intervals, taking the mean

value for each interval. The mean wind velocity was calculated from its frequency of occurrence, expressed in percentages, according to the formula:

$$\bar{u} = \frac{\sum n_i u_i + n_c}{100} \quad [\text{cm s}^{-1}]$$

where n_c — the frequency of occurrence of calms. The materials were prepared for mean monthly values in January and July, embracing the sea areas for which the above results were available. The computations were carried out on an electronic digital computer according to the programme for an algorithm elaborated with the conceptual assumptions and general expression (6) presented above.

The Schlichting formula [28] was adopted to estimate the roughness of an aerodynamic sea surface, the improvements in the formula being elaborated by Wu [33]. The formula was modified taking into account $\bar{h}_f$ — the mean height characteristic of the wind waves. The $\bar{h}_f$ value was determined from empirical data of the dependence of this magnitude on the wind velocity. Hence, the relation for z_o was used in the following form:

$$z_0 = \frac{3 \cdot 10^{-3} \bar{h}_f}{\exp(\varkappa / \sqrt{c_{10}})} \qquad (14)$$

where $\varkappa$ — the Kármán constant, $c_{10} = 0.5 \times 10^{-3} \sqrt{(u^2_{10}/u^{2*})}$ for $u_{10} < 15$ m s^{-1}. On applying the above c_{10} value, equation (14) enabled the whole interval of mean monthly wind velocities to be taken into account while computing z_o and not only the smooth surface, i. e. for $z_o < \delta v$.

It can be inferred from numerous experimental data that the effective interaction of the wind occurs mainly together with elements of the small-period component of undulation. Significant tangent stresses in the state of non-stormy undulation are related mainly with short-waves and ripples of the capillary wave type. Under such conditions, parameter $z_o \sim \delta v$ i. e. the sea surface behaves as an aerodynamically rough one, and Re_s reaches the critical value, which means the beginning of effective emission. The introduction of $\bar{h}_f$ into equation (14) also enabled the influence of ripples to be taken into account simultaneously — the total sea surface area changes together with $\bar{h}_f$, hence, the general number of ripples on the undulating area also changes.

The z_o values computed from equation (14) are compared with the z_o values computed for the ocean according to the Deacon-Webb equation [7]. The results (in cm) are presented in the following table:

	at wind velocities (cm s^{-1})			
	100	300	400	800
z_o according to ref. [7]		0.012	0.014	0.04
z_o according to eq. (14)	0.003	0.033	0.067	0.200

The rapid increase in the z_o values computed from (14), with the wind velocity, does not explain the difficulties related to the determination of the z_o parameter for the sea, it does, however, justify the curves for the q dependence on u, computed for sea salt particles (Fig. 2) on the basis of equation (10).

The Deacon-Webb formula [8] was used to calculate the u values:

$$u_*^2 = \frac{u_{10}^2 + 7 \cdot 10^{-4} u_{10}^3}{1000} \quad [\text{cm}^2\ \text{s}^{-2}] \qquad (15)$$

Formula (15) was obtained from an analysis of the vertical distribution of wind velocity over the sea surface, and on taking the relation $c_D = \frac{u_*^2}{u_{10}}$ it enabled the determination of the dimensionless drag coefficient (c_D) for a standard level of $z = 10$ m above the sea level.

On calculating the flux Q_{10} for $z = z_o$, the characteristic lokal k values had to be taken into account. They were partially obtained from an analysis of the dependence of the sea salt volumetric concentration in tre near-water air on the wind velocity. Accordingly, experimental material was collected from two regions — the central part of the Altantic [26] and the open Baltic areas [12]. The comparison of the results (Fig. 2) enabled the determination of the k coefficient from the relation:

$$k = \alpha \frac{\sqrt{\varrho_p}}{\sqrt[4]{(\varrho_w - \varrho_p)}} \qquad (16)$$

For the ocean, $\alpha = 2.2 \times 10^{-9}$ was obtained. Simultaneously, the value of this constant for the Baltic was found to be much lower (0.5×10^{-9}). In principle, α was determined from measurements of NaCl particles in the near-water atmospheric layer.

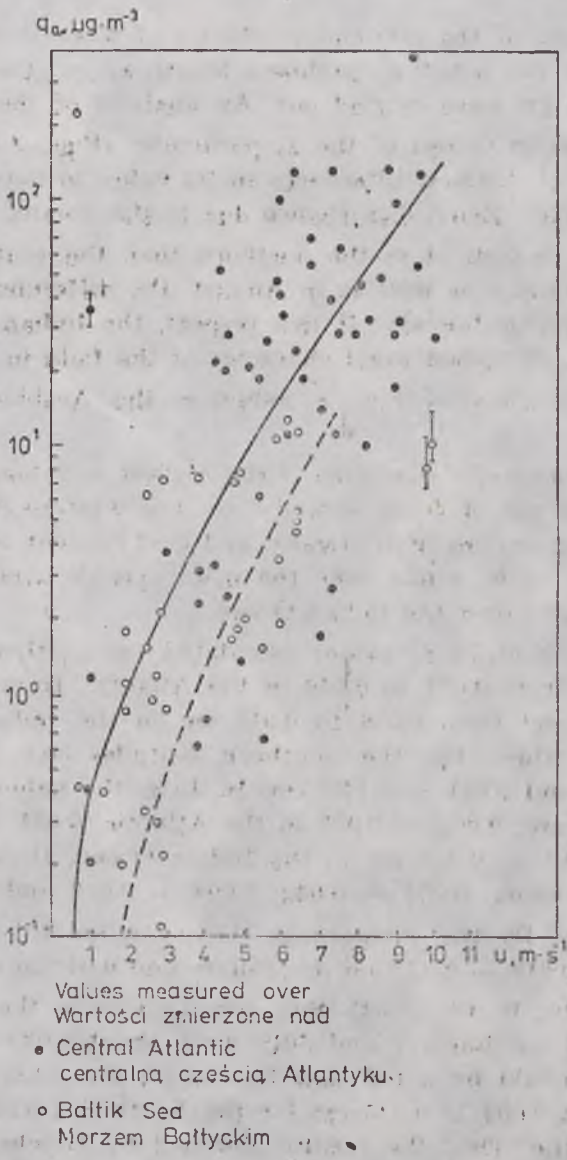

Fig. 2. Concentration of sea salt in the near-water air (mean 10 m above sea level) depening upon the wind velocity, according to measurements carried out in the central part of the Atlantic (black dots) and in the Baltic Sea (empty dots)
Rys. 2. Koncentracja soli morskiej w powietrzu przywodym (średnio 10 m nad poziomem morza) w zależności od prędkości wiatru według pomiarów w centralnej części Atlantyku (punkty czarne) i na Bałtyku (punkty puste)

4. PHYSICAL CHARACTERISTICS OF INTERACTION

4.1. Roughness length

The computations of the two characteristics of interaction between the atmosphere and the sea, the roughness length z_o and the dimensionless dynamic factor ξ_{10} were carried out. An analysis of the spatial distribution of the mean values of the $\bar{z}_o$ parameter (Figs. 3 and 4) showed the occurrence of distinct differences in its value to have only a general zonal character. Zonal disturbance due to the oceanic centre of high $\bar{z}_o$ values is more distinct in the northern than the southern latitudes. It occurs in January, as well as in August, the differences being much more pronounced in January. It this respect, the Indian Ocean differs, and the slightly disturbed zonal character of the field in January changes into three centres of high $\bar{z}_o$ values — the Arabian, Bengal and Australian.

The occurrence of the centres of the highest $\bar{z}_o$ values in the oceans is due to: 1) areas of storm activity in the western transfer zones, especially in the regions of the warm and cold current interface, 2) intensification of trade winds over the open oceanic areas, 3) monsoon circulation activity over the Indian Ocean.

The mean monthly $\bar{z}_o$ values calculated for northern latitudes in January range from 0.001 to 0.049 in the Atlantic, from 0.001 to 0.063 in the Pacific and from 0.006 to 0.012 cm in the Indian Ocean. The corresponding values for the southern latitudes are 0.001 — 0.028, 0.002 — 0.045 and 0.003 — 0.037 cm. In July, the values for the northern latitudes are: 0.001 — 0.027 in the Atlantic, 0.001 — 0.023 in the Pacific and 0.001 — 0.048 cm in the Indian Ocean, those for the southern latitudes being: 0.004 — 0.042, 0.004 — 0.068 and 0.001 — 0.045 cm, respectively. By the comparison, the mean monthly $\bar{z}_o$ values for the Baltic are: 0.019 — 0.031 cm in January and 0.04 cm over the whole sea area in July. In the North Sea areas adjoining the Baltic the z_o values obtained for January and July were about 0.020 and 0.010, respectively. It should be noted that Brocks [6] also obtained values of z_o ranging from 0.004 to 0.025 cm for the North Sea and the northern part of the Baltic. Thus the results obtained by Brocks for the same area conform, in principle, with the above, despite the different approach to the problem. This statement supports the conclusion that a good approximation of the fields of $\bar{z}_o$ values was obtained for the World Ocean.

Fig. 3. Roughness length field ($\overline{z_0}$, cm) in January.
Rys. 3. Pole parametru szorstkości ($\overline{z_0}$, cm) w styczniu.

Fig. 4. Roughness length field ($\bar{z}_0$ cm) in July.
Rys. 4. Pole parametru szorstkości (z_0 cm) w lipcu.

4.2. Dimensionless emission factor

The mean values of the parameter $\bar{\xi}'_{10}$ calculated from the mean monthly $\bar{z}_0$ values and other oceanographic elements, became the basis for obtaining approximate spatial distributions of this characteristic (Figs. 5 and 6). The analysis of the $\bar{\xi}'_{10}$ field enabled the discovery of the distinct occurrence of several areas of maximum capacity for marine aerosol emission and spatial dispersion in the oceans.

The predominance of extensive source regions forming in the middle and tropical latitudes in the Atlantic and Pacific is characteristic of January. The former area, as opposed to the latter, deviates from the zonal configuration, reaching much further north. Simultaneously, in the middle southern latitudes one can also distinguish two predominant but markedly weaker source regions, one in the Indian Ocean and the second — in the Pacific. On the other hand, in the case of the approximately general zonal character of the field, only small centres of slightly emission capacity can be found in the northern zone of the trade winds.

In July the predominance of the northern centres disappears. Simultaneously, the occurrence of a predominant emission source in the form of a vast zone situated in the middlesouthern latitudes was observed. This zone stretches across the three oceans and it shows the highest emission capacity in the Pacific, particularly in the area between New Zealand and Tierra del Fuego. In the other Pacific and Atlantic zones, a lack of predominant source regions was found, with the exception of the trade wind southern zones, where only a slight predominance of several small source regions can be observed. The Indian Ocean was the only exception, for which a distinct occurrence of two not very vast source regions can be observed in the Arabian and Bengal Seas.

The degree of approximation of the results obtained was verified basing on regional characteristics, taking the Baltic as the main example. The investigations showed that as compared with the whole field, in January the Baltic constitutes something of an extension of the north-Atlantic source region, the predominant $\bar{\xi}'_{10}$ values being found mainly in the northern part of the Baltic. Such situation is usually maintained throughout the whole year, this being confirmed by the mean annual isolines of $\bar{\xi}'_{10}$ obtained for this region over a period of many years (Fig. 7). In January, the $\bar{\xi}'_{10}$ values found for the parts of the Atlantic adjoining the Baltic are included in the interval of $(1000 - 2000) \times 10^{-12}$, which is also consistent with the results of detailed measurements of the $\bar{\xi}'_{10}$ field, carried out in the Baltic Sea [11]. In ad-

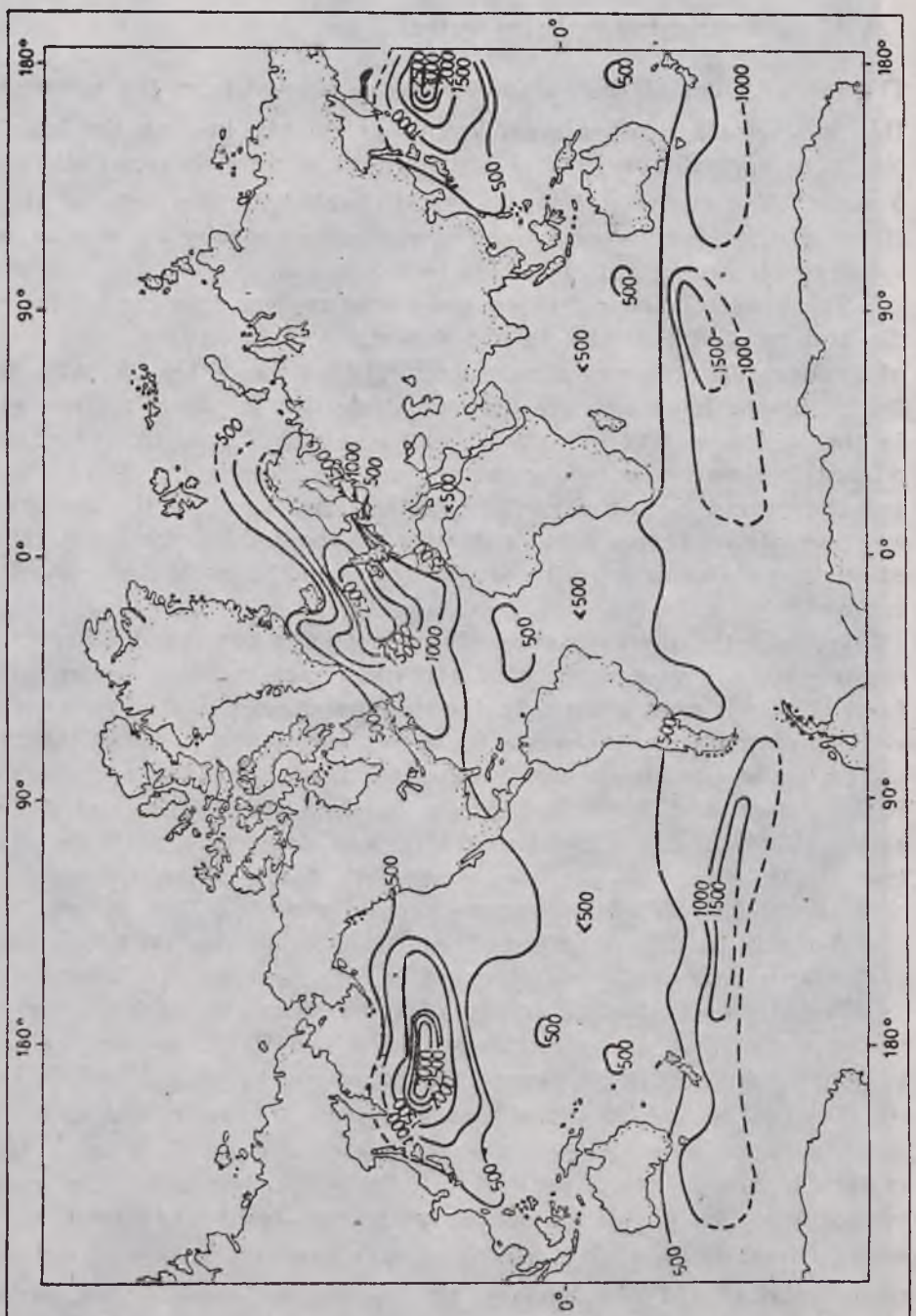

Fig. 5. Field of the dimensionless wind factor ($\overline{\Xi'_{10}} \times 10^{12}$) in January.
Rys. 5. Pole bezwymiarowego czynnika wiatrowego ($\overline{\Xi'_{10}} \times 10^{12}$) w styczniu.

Fig. 6. Field of the dimensionless wind factor ($\overline{\Xi'}_{10} \times 10^{12}$) in July.
Rys. 6. Pole bezwymiarowego czynnika wiatrowego ($\overline{\Xi'}_{10} \times 10^{12}$) w lipcu.

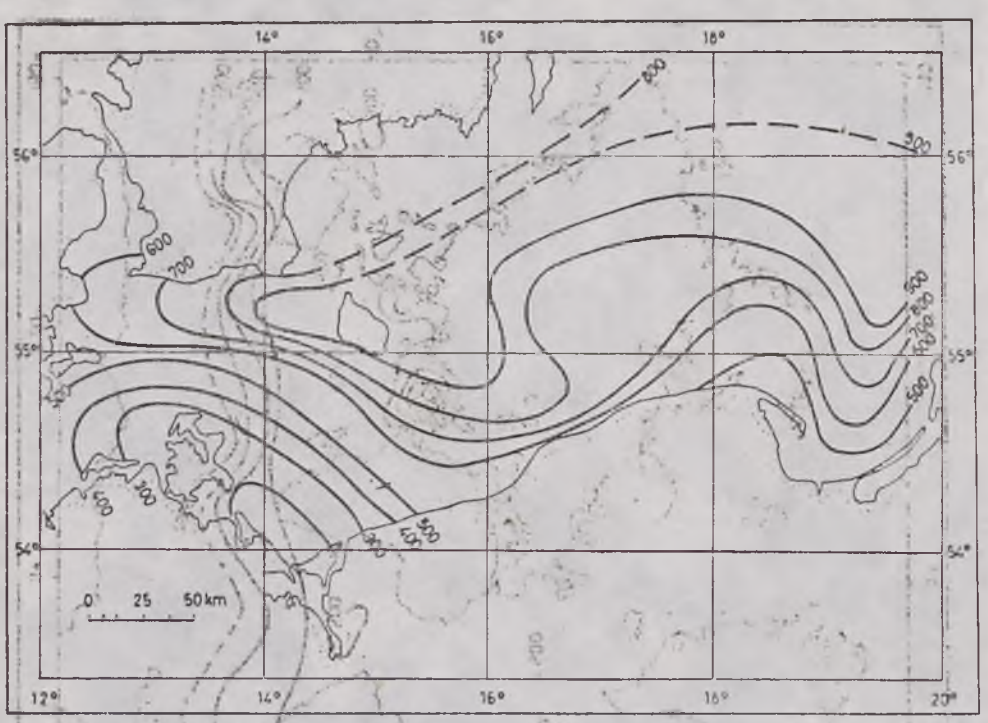

Fig. 7. Mean annual field of the dimensionless wind factor ($\bar{\xi}'_{01} \times 10^{12}$) for the Baltic Sea

Rys. 7. Średnie roczne pole bezwymiarowego czynnika wiatrowego ($\bar{\xi}'_{10} \times 10^{12}$) na Morzu Bałtyckim.

dition, a lack of predominance of the emission capacity was confirmed for the Baltic during the warm half of the year, for which $\bar{\xi}'_{10} = (100—350) \times 10^{-12}$ was obtained. As results from the present computations, extremely low values of the $\bar{\xi}'_{10}$ parameters are observed in the Baltic in July ($\bar{\xi}'_{10} = 48 \times 10^{-12}$ for the southern and northern parts of the sea). These values are several times lower than those obtained for the Atlantic in July at latitudes level with those of the Baltic Sea. Similar values of $\bar{\xi}'_{10}$ at such latitudes can only be found in the region between Iceland and the eastern coasts of Greenland.

4.3. Sea-salt particle flux

Basing on the distribution of the $\bar{\xi}'_{10}$ values obtained above, the sea-salt particle emission field could be computed, taking into account the surface water salinity. Thus the fields of the mean monthly $\bar{Q}_{10}$ values for sea-salt particles were obtained (Figs. 7 and 8).

Fig. 8. The sea-salt particle emission field ($\overline{Q}_{10}$, ng cm^{-2} s^{-1}) in January.
Rys. 8. Pole emisji cząstek soli morskiej ($\overline{Q}_{10}$, ng cm^{-1}) w styczniu.

From the comparison of spatial distributions of mean values of the parameters $\bar{\xi}_{10}$ and Q_{10} one can easily note that the character of the distribution of main source region of the $\bar{Q}_{10}$ component is essentially similar to that of the emission capacity field calculated for the whole of the World Ocean (Figs. 5 and 6). Here, the field of the $\bar{\xi}'_{10}$ parameter is the basic one, this undergoing only slight modification under the influence of the water salinity field. Geographical distribution of the predominant source regions remains practically the same, the outline of the boundaries of main centres of the sea-salt particle emission being more pronounced. Differences can be noted particularly in the trade wind zones — in January in northern and in July in the southern latitudes. In the latter period, the extensive and distinctly limited source region predominates in the trade wind zone in the southern part of the Pacific.

Simultaneously, a distinct predominance of source regions occurs in the middle geographical latitudes of both hemispheres. The Pacific Ocean is particularly distinctive in this respect, the region between 30° and 60°S spreading far to the east of New Zealand. Correspondingly, the second centre spreads zonally in the middle northern latitudes whereas the Atlantic has only one main source region which stretches more between about 40° and 60° N. The Baltic, on the other hand, is not a source region, being only a sink region with respect to the Atlantic centre of sea-salt particle emission.

4.4. Zonal distribution of water drop emission and mechanical evaporation

The problem of so-called mechanical evaporation (occurring from the surface of drops emitted from the sea) is connected with the spatial distribution of the marine aerosol source and sink regions. The problem concernes one of the important components of the macroscale budget of water circulation between the sea and the atmosphere, which have been wrongly neglected so far. An attempt can be made to calculate this component according to the relation:

$$Q'_{10} = c_Q c_D \varrho_w u_{10} \xi_{10} \left(1 - \sum_{k=1}^{n} q_k\right) \qquad (17)$$

where Q'_{10} — total flux of mechanical evaporation at a standard height of 10 m above sea level,

$\sum_{k=1}^{n} q_k$ — relative share of sea salts in the sea surface layer.

Surface s of spherical particles at time t can be calculated from the magnitude of the water dust flux (Q_o) when the number of drops and their radius r are known. The dependence of s on t for clear water drops is approximately linear ($\frac{ds}{dt} = \text{const}$), the deviation from the time axis becoming noticeable as the drops become smaller. The evaporation rate decreases with the increase of the drop curvature, as evapiration time t is equal to $t = c \frac{E_r - e}{r_2 - r_1}$, the pressure of saturated water vapour being $E_r = E^\infty + \Delta E_r$

where

E^∞ — pressure of water vapour above the flat surface of the water,

ΔE_r — correction taking into account the influence of the convex curvature (for drops of $r = 10^{-4}$ cm, $\Delta E_r = 0.1\%$ of E^∞).

On the other hand, above the solution, $E_{rr} = E^\infty - \Delta E_{rr}$, which causes an increase in time t. To this should be added the presence of monomolecular layers of natural or often anthropogenic origin on the drop surface, which inhibit evaporation. Non-volatile admixtures which are often present already in the initial mass of drops or captured by the drops during coagulation with the dust particles, constituting the characteristic aerosol background in the atmosphere, may even halt the further evaporation process as their concentration in the diminishing drops increases. Apart from the influence of the evaporation of drops, these admixtures, while reducing the surface tension of the sea, may indirectly influence the evaporation by attenuation of the water dust flux, Q_o. These problems have not, however, been explained as yet, when considering the true conditions at sea. Thus when calculating Q'_{10} according to (17), it is possible to gain some knowledge of the possible maximum fluxes of mechanical evaporation when taking into account the surface essential to evaporation [25].

It can be inferred from the analysis of zonal distribution of the Q'_{10} values calculated for January and July (Figs. 10 and 11) that the evaporation surface of the water drops emitted from the sea, being an additional surface which supplies water vapour to the atmosphere, increases predominantly at middle northern and southern latitudes. These values describe potential fluxes of mechanical evaporation. They should also be influenced by the temperature and relative humidity of the atmospheric air.

Taking as a base the sets of drops of $\bar{r} \sim 12.6$ μm transferred from the Atlantic Ocean to the Baltic [12], the surface area of mechanical

Fig. 9. The sea-salt particle emission field ($\overline{Q}_{10}$ ng cm^{-2} s^{-1}) in July
Rys. 9. Pole emisji cząstek soli morskiej ($\overline{Q}_{10}$, ng cm^{-2} s^{-1}) w lipcu

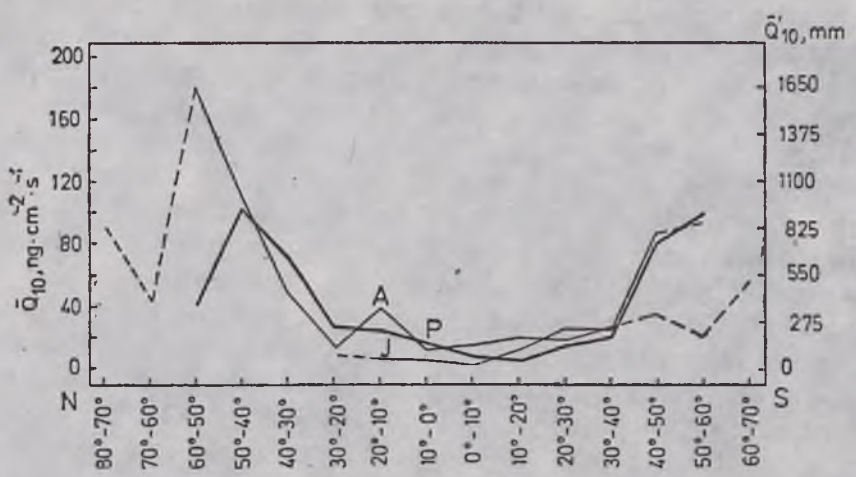

Fig. 10 Mean distribution of particle emission and that of the potential fluxes of mechanical evaporation from the oceans (mm/year) in latitudinal profile, calculated for January (A — Atlantic, P — Pacific, I — Indian Oceans)

Rys. 10. Średni rozkład emisji cząstek i potencjalnie możliwych strumieni parowania mechanicznego z oceanów (mm/rok) w przekroju południkowym — obliczony dla stycznia (A — Atlantyk, P — Pacyfik, I — Ocean Indyjski)

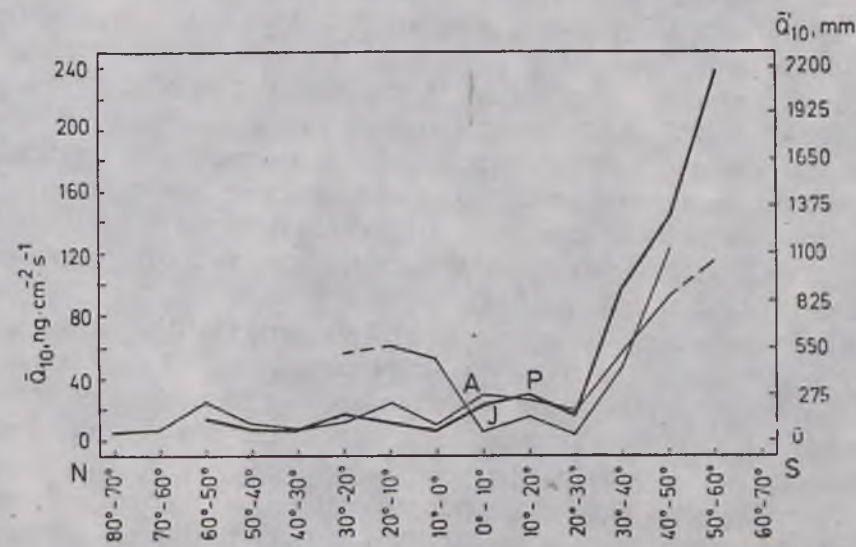

Fig. 11. Mean distribution of particle emission and that of the potential fluxes of mechanical evaporation from the oceans (mm/year) in latitudinal profile, calculated for July

Rys. 11. Średni rozkład emisji cząstek i potencjalnie możliwych strumieni parowania mechanicznego z oceanów (mm/rok) w przekroju południkowym — obliczony dla lipca

evaporation was calculated to represent an average of 0.5% of the sea surface area. It should be emphasized that the calculations were carried out on the basis of the analysis of drop size distribution for drops belonging to the group of giant particles. Although the presence of the more numerous smaller particles increases the surface, their evaporation time is markedly prolonged. Therefore for the World Ocean surface area, amounting to 361.06×10^6 km^2 without the shelf ice area, the surface area of mechanical evaporation thus calculated is approximately equal to 1.81×10^6 km^2. For the zones with the lowest (10°—20° S) and highest (40°—50° N) values of Q'_{10} in January in the Pacific for which the typical mean wind velocities are 5.3 and 8.9 m s^{-1}, respectively, the surface areas of mechanical evaporation were calculated to be 0.08 and 0.83% of the sea surface area (27×10^3 and 125×10^3 km^2, respectively). It is imperative to take the share of these values into account when improving long-term weather forecasts.

5. CONCLUSIONS

The calculated fields of the parameters $\bar{z}_0$ and $\bar{\xi}'_{10}$ constituting the basic physical characteristics of the interaction between the atmosphere and the sea, afforded an approximate orientation as to the geographical distribution and significance of the main marine source regions. Such investigations are indispensable in the explanation of the peculiarities connected with the water budget and the substances contained in water, from the viewpoint of their circulation in macroscale and synoptic cycles corresponding to the first and second degree cycles (in this paper the first degree cycle comprises the ocean-atmosphere-land circulation while the second degree cycle denotes the marine source region-atmosphere-marine sink region cycle).

In investigating the geographical distribution of the emission areas, only a general outline of the two-dimensional field of basic anemoaerosol characteristics above the ocean surface has been obtained. The third dimension, i.e. time, was taken into account only in respect of months falling in two seasons of the year — cold and warm. One could not count on the possibility of carrying out the investigations for the purpose of obtaining detailed results. The scale of the investigations planned was also of great importance. The results obtained are therefore approximate, nevertheless they may afford valuable information that can be useful in the meteorology of atmospheric suspensions distribution, as well as in investigations on particle exchange and transfer in the four-dimensional coordinate system.

The author wishes to thank mgr Danuta Wielbińska and mgr Krzysztof Lubomirski for their help in the selection of material and the organization of the numerical data processing.

Czesław GARBALEWSKI

Polska Akademia Nauk
Zakład Oceanologii w Sopocie

ŚREDNI ROZKŁAD PRZESTRZENNY PODSTAWOWYCH FIZYCZNYCH CHARAKTERYSTYK I ŹRÓDŁOWCH OBSZARÓW EMISJI CZĄSTEK Z POWIERZCHNI OCEANÓW

Streszczenie

Badano rozkład na oceanach względnych obszarów źródłowych i ujściowych z punktu widzenia tzw. mechanicznego parowania wody. Na podstawie koncepcji warstwy emisji złożonej z podwarstw transformacji i przenoszenia cząstek opracowano model opisujący emisję cząstek z otwartych obszarów morza (poza efektem stref przyboju). Parametry modelu (w tym współczynnik emisji c_ρ, zależny głównie od gestości powietrza i wody morskiej, współczynnik oporu c_D, parametr szorstkości z_o i bezwymiarowy czynnik dynamiczny $\xi = \frac{Re_s}{M}$, gdzie Re_s — liczba Reynoldsa dla powierzchni, $M = \frac{u_{10}}{u_*}$, u_{10} — prędkość wiatru na standardowej wysokości 10 m, u_* — prędkość tarcia) określano z wieloletnich danych zawartych w zestawieniach poświęconych klimatom mórz i w atlasach morskich.

Dokonano pierwszej próby uzyskania podstawowego zarysu oceanograficznych pól średnich miesięcznych wartości parametru szorstkości ($\bar{z}_o$), bezwymiarowego czynnika wiatrowego ($\bar{\xi}'_{10}$) i strumieni soli morskiej ($\bar{Q}_{10}$). Stwierdzono, że występowanie ośrodków najwyższych wartości $\bar{z}_o$ na oceanach wiąże się: 1) z obszarami działalności sztormowej w strefach zachodniego przenoszenia, 2) z intensyfikacją pasatów nad otwartymi obszarami oceanicznymi i 3) z działalnością cyrkulacji monsunowej na Oceanie Indyjskim. W związku z tym dominowanie rozległych źródeł emisji cząstek marygenicznych uzyskano w styczniu w pasie średnich szerokości na Atlantyku i na Pacyfiku, w lipcu zaś — na średnich szerokościach południowych, w szczególności na obszarze między Nową Zelandią a Ziemią Ognistą. Obliczone wartości parowania mechanicznego $\bar{Q}'_{10}$ wahały się od 0,08 do 0,83% w stosunku do parowania odbywającego się bezpośrednio z powierzchni morza. Najwyższe potencjalne wartości $\bar{Q}'_{10}$ uzyskano dla stref zachodniego przenoszenia. Stwierdzono, że Ocean Indyjski znacznie różni się pod względem rozkładu $\bar{Q}_{10}$ i $\bar{Q}'_{10}$.

Morze Bałtyckie w styczniu tworzy jakby przedłużenie północnoatlantyckiego pola parametru $\bar{\xi}'_{10}$, przy czym w orbitę dominujących wartości $\bar{\xi}'_{10}$ wchodzi głównie północna część Bałtyku. W lipcu wartości $\bar{\xi}'_{10}$ na Bałtyku są kilkakrotnie niższe od obserwowanych na tych samych szerokościach na Atlantyku. Generalnie Morze Bałtyckie nie stanowi obszaru źródłowego, tylko jest obszarem ujściowym w stosunku do atlantyckiego ośrodka dominowania emisji mas aerozolu marygenicznego.

REFERENCES

1. Blanchard D. C., *The electrification of the atmosphere by particles from bubbles in the sea*, Progress in Oceanogr., Vol. 1, 1964.
2. Blanchard D. C., *The Oceanic Production Rate of Cloud Nuclei*, J. Rech. Atm., Vol. IV, 1969, No. 1.
3. Blanchard D. C., A. H. Woodcock, *Bubble formation and modification in the sea and its meteorological significance*, Tellus, IX, 1957.
4. Bellashova M. A., *O raspredelenii aerozolei nad moryami*, Trudy GGO, 1973, wyp. 293.
5. Blinov I. K., *O postuplenii morskikh solei v atmosferu i o znachenii vetra v solevom balanse Kaspiiskogo morya*, Trudy GOIN, 1950, wyp. 15.
6. Brocks K., L. Krugermeyer, *The hydrodynamic roughness of the sea surface*, Inst. f. Radiometeor. u. Maritime Meteorologie 1970, Rep. No. 14, Hamburg University IAPSO Meeting in Moscow, July-August 1971, Naval Undersea Center, San Diego, Calif. 1972.
7. Deacon E. L., E. K., Webb, *Small scale interactions. The Sea* (ed.M.H.Hill), Vol. 1, New York 1962.
8. Deacon E. L., P. A. Sheppard, E. K. Webb, *Wind profiles over the sea surface*. Austr. J. Phys., Vol 9, 1956, No. 4.
9. Duce R. A., A. H. Woodcock, *Difference in chemical composition of atmospheric sea salt particles produced in the surf zone and on the open sea in Hawaii*, Tellus, XXIII, 1971.
10. Eriksson E., *The yearly circulation of chloride and sulfur in nature; meteorological, geochemical and pedological implications*, Part I, Tellus XI, 1959.
11. Garbalewski C., K. Kwiecień, *On the conditions of emission and transfer of sea-concentrates in the southern Baltic region*, Proc. of IX Conf. of Baltic Oceanogr., Kiel 1974; O warunkach emisji i przenoszenia koncentratów morskich w rejonie południowego Bałtyku, Wiad. Meteorol. i Gosp. Wodn., I, 1974, nr 4.
12. Garbalewski C., *Dynamika aerozolowej wymiany masy na otwartych obszarach Bałtyku*, [Dynamics of aerosol mass exchange on the open Baltic areas]. Mater. Bad. IMGW, Ser. Hydrol. i Oceanol., Warszawa 1977.
13. Garrett W. D., *The influence of monomolecular surface films on the production of condensation nuclei from bubbled sea water*. J. Geophys. Res., Vol. 73.

14. Garretson G. A., *Bubble transport theory with application to the upper ocean.* J. Fluid Mech. Vol. 59, 1973, No. 1.
15. Junge C. E., *The size distribution and aging of natural aerosols as determined from electrical and optical data of the atmosphere.* J. Meteor., 12, 1955.
16. Junge C. E., *Radioaktivnye aerozoli. Yadernaya geofizika,* Moskva 1964.
17. Karol I. L., *Radioaktivnye izotopy i global'nyi perenos v atmosfere,* Leningrad 1972.
18. Katsuhiro Kikushi, Shogo Yaura, *Observations of giant-salt particles over the ocean from Tokyo to Syova Station,* Antarctica. J. Met. Soc. Japan. Ser. II, Vol. 48, 1970, No. 4.
19. Kutateladze S. S., *Pristennaya turbulentnost,* Novosibirsk 1973.
20. *Marine Climate Atlas of the World,* 1965, U.S. Navy, Washington D.C.
21. Mason B. J. *Bursting of air bubbles at the surface sea water.* Nature, 174, 1954.
22. Monahan E. C., *Sea spray as a function of low elevation wind speed.* J Geophys. Res., Vol. 73, 1968, No. 4.
23. Moore D. J., B. J. Mason, *The concentration, size distribution and production rate of large salt nuclei over oceans.* Quarst. J. R. Met. Soc. Vol. 80, No. 346, 1954.
24. *Morskoi atlas, Fiziko-geograficheskii,* t. 2, Moskva 1953.
25. Garbalewski C., L. Balcer, J. Kowalewski, K. Lubomirski, *O strefowym rozkładzie parowania mechanicznego i emisji jąder kondensacji z oceanów.* [On zonal distribution of mechanical evaporation and emission of the condensation nuclei from the oceans], Stud. i Mater. Oceanol., 1978, No 26.
26. Kientzler C. F., A. B. Arons, D. C. Blanchard, A. H. Woodcock, *Photographic investigation of the projection of droplets by bubbles bursting at a water surface,* Tellus, VI,1954.
27. Bortkovskii R. S., E. K. Byutner, S. P. Malevskii-Malevich, L. J. Preobrazhenskii, *Procesy perenosa vblizi poverkhnosti razdela okean-atmosfera.* Gidrometeoizdat., Leningrad 1974.
28. Schlichting J., *Boundary layer theory.* McGraw Hill, New York 1955.
29. Toba Y., *On the giant sea-salt particles in the atmosphere.* Part I: *General features of the distribution,* Tellus, XVII, 1965.
30. Toba Y., *On the giant sea-salt particles in the atmosphere.* 2: *Theory of vertical distribution in the 10 m layer over ocean,* Tellus, XVII,1965.
31. Woodcock A. H., *Smaller salt particles in oceanic air and bubble behaviour in the sea,* J. Geophys. Res., Vol. 77, 1972, No. 27.
32. Woodcock A. H., *Salt nuclei in marine air as a function of altitude and wind force,* J. Met., 1953, No. 10.
33. Wu J., *Wind stress and surface roughness at air-sea interface,* J. Geophys. Res., Vol. 74, 1969, No. 2.
34. Wu J., *Spray in the atmospheric surface layer; laboratory study.* J. Geophys. Res., Vol. 78, 1973, No. 3.